UDK 546.17:546.293:67.017:621.793:669.058.6:539.92
Original scientific article/Izvirni znanstveni članek

ISSN 1580-2949
MTAEC9, 55(6)789(2021)

EFFECT OF THE N_2/Ar FLOW RATIO ON THE MICROSTRUCTURE AND MECHANICAL PROPERTIES OF TiSiCN COATINGS

VPLIV RAZMERJA MED DUŠIKOM IN ARGONOM V PLINSKI MEŠANICI NA MIKROSTRUKTURO IN MEHANSKE LASTNOSTI PREVLEK NA OSNOVI TiSiCN

Jin Wang[1*], Mengting Wang[1], Yongqiang Wang[1], Dayan Ma[2], Hao Li[2]

[1]School of Mechanical and Automotive Engineering, Qingdao University of Technology, Qingdao 266520, China
[2]School of Materials, Xi'an Jiaotong University, Xian 710000, China

Prejem rokopisa – received: 2021-07-07; sprejem za objavo – accepted for publication: 2021-09-10

doi:10.17222/mit.2021.213

TiSiCN coatings were prepared with the multi-arc ion plating and magnetron sputtering technique. The effect of the N_2/Ar flow ratio on the properties of TiSiCN coatings was studied using scanning electron microscopy (SEM), X-ray diffraction (XRD), X-ray photoelectron spectroscopy (XPS) and a friction and wear tester (UMT-3). With an increase in the N_2/Ar flow ratio, the number of large particles on the surface first increases and then decreases. The intensity of the TiN (200) diffraction peak increases gradually, while the grain size first decreases and then increases. A TiSiCN coating consists of Ti (N, C) nanocrystallites, amorphous SiC, Si_3N_4 and carbon. When the N_2/Ar flow ratio is 5 : 1, the coating exhibits the highest hardness and excellent wear resistance.

Keywords: TiSiCN; multi-arc ion plating, magnetron sputtering, N_2/Ar flow ratio, mechanical properties, tribological properties

Avtorji v članku opisujejo pripravo trdih prevlek na osnovi TiSiCN s tehnikama večobločnega ionskega platiranja in magnetronskega napraševanja. Raziskovali so vpliv razmerja med dušikom in argonom (N_2/Ar), uporabljenega v pretoku zaščitnega plina, na lastnosti izdelanih TiSiCN prevlek. Študije so izvajali s pomočjo vrstične elektronske mikroskopije (SEM), rentgenske difrakcije (XRD), rentgenske fotoelektronske spektroskopije (XPS) in tornih ter obrabnih preizkusov na univerzalnem večfunkcionalnem trenjsko-obrabnem testerju (UMT-3; angl.: Multifunctional friction and wear tester). S povečanjem vsebnosti dušika v pretakajoči se plinski mešanici, je število velikih delcev na površini najprej naraslo in nato padlo. Intenziteta TiN (200) difrakcijskega pika je postopno naraščala, velikost kristalnih zrn pa se je najprej zmanjševala nato pa postopno naraščala. Ugotovili so, da so izdelane TiSiCN prevleke sestavljene iz nanokristalov Ti(N,C), amorfnega SiC, Si_3N_4 in ogljika. Ko je bilo v plinski mešanici uporabljeno razmerje N_2/Ar 5 : 1 je imela prevleka največjo trdoto in odlično odpornost proti obrabi.

Ključne besede: prevleke na osnovi TiSiCN, več-obločno ionsko platiranje, magnetronsko napraševanje, razmerje med dušikom (N_2) in argonom (Ar) v pretoku plinske mešanice, mehanske in tribološke lastnosti

1 INTRODUCTION

Hard coatings are widely used in the machinery industry because of their high hardness, good wear resistance and excellent mechanical properties. The TiN coating, being the first-generation hard coating, has poor oxidation resistance and low hardness. An addition of Si can improve the stability and mechanical properties of the TiN coating.[1–4] Zhu et al.[5] prepared a TiSiN coating with arc ion plating and found that the coefficient of friction decreases with an increase in the temperature. The coating had a large number of cracks at 500 °C and oxygen entered the coating, causing oxidation. The process of a coating failure was divided into three parts. The first part included a thermal expansion and stress increase; then the coating was broken and initially oxidized; and the last part included oxygen penetration and coating failure. Marchin et al.[6] prepared a TiSiN coating with the industrial cathodic arc physical vapor deposition. With an addition of carbon, the surface hardness increased, the residual stress level and the friction coefficient reduced, and the life of the coating improved greatly.

There are also many reports on the research of TiCN and other ternary-component coatings. TiCN coatings attracted widespread attention in scientific research and industrial applications due to their excellent mechanical properties.[7–10] Liu et al.[11] prepared TiCN coatings on cermets and cemented carbide tools using chemical vapor deposition. The results showed that the coating prepared on cemented carbide was denser and had a shorter life span than that deposited on cermet. Coated cermets had a longer tool life and lower toughness. Excellent diffusion and binding-force resistance at high temperatures enhanced the surface quality of a workpiece. Sun et al.[12] prepared a TiCN coating on high-speed steel using multi-arc ion plating. The study found that with an in-

*Corresponding author's e-mail:
jinwangqtech@163.com (Jin Wang)

crease in the carbon content, the mechanical properties improved significantly, the hardness increased gradually, and the friction coefficient decreased gradually.

In recent years, researchers tried to overcome the shortcomings of the ternary-coating performance using chemical vapor deposition, magnetron sputtering, arc ion plating and other methods.[13–16] In particular, TiSiCN nanocomposite coating can combine the advantages of TiSiN coating and TiCN coating to improve the mechanical and tribological properties of coatings. Ma et al.[17] prepared a TiSiCN coating using the pulse-enhanced vacuum-arc evaporation technology. When the target-substrate distance was increased from 200 mm to 300 mm, the average substrate current was increased by 53.8 % and the deposition rated was increased by 36.4 %. The microstructure was denser, and the corrosion resistance and wear resistance were better. Wang et al.[18] prepared a TiSiCN coating on a Ti6Al4V substrate. Studies showed that wear was the main reason for the coating failure, and the coating with a high carbon content exhibited excellent lubrication and wear resistance in the atmosphere. When a channel through the coating was formed between the substrate and the surface, the cathodic protection potential played a negative role in preventing a coating failure.

There have been sufficient studies to prove that the temperature, N_2 flow rate and bias voltage are important parameters in a deposition process, and that they have significant effects on the morphology, composition, microstructure, oxidation resistance, mechanical properties and tribological properties of a coating.[19–22] Li et al.[23] obtained diamond films of different thicknesses by adjusting the N_2/Ar flow ratio. The results showed that with an increase in the N_2/Ar flow ratio, the Cr (Si) phase in the interlayer decreased gradually, and the thickness of the diamond film increased. When the proportion reached 50 %, the intermediate layer was composed of the (Cr, Si) N phase, and the film thickness was the largest. When the ratio was greater than 50 %, a $(Cr, Si)_2N$ phase appeared, and the cell density was low. Carbon atoms could diffuse inward easily, reducing the thickness of the diamond film. Yang et al.[24] prepared a ScAlN coating using DC reactive magnetron sputtering. The results showed that the N_2/Ar flow ratio was an important controlling factor in the sputtering process. When the N_2/Ar flow ratio was 3.3 : 7, the best crystallization state and the minimum surface roughness were obtained. With the increase in the N_2/Ar flow ratio, the crystal quality first increased and then decreased, and the resistivity and dielectric constant first increased and then decreased. Compared with the AlN coating, the ScAlN coating has higher resistivity and dielectric constant. There are few studies on the effect of the N_2/Ar flow ratio on the microstructure and mechanical properties, and even fewer studies on a TiSiCN coating, even though its preparation technology is relatively simple. A coating prepared with multi-arc ion plating has good film/substrate interfacial binding force, and a coating prepared with magnetron sputtering has good compactness. The composite technology of multi-arc ion plating and magnetron sputtering can combine the advantages of the two.[25–27] Therefore, this research combined the two technologies, multi-arc ion plating and magnetron sputtering, to prepare TiSiCN coatings with different N_2/Ar flow ratios on the surface of H13 die steel. The effects of the N_2/Ar flow ratio on the microstructure and properties of the coatings were studied.

2 EXPERIMENTAL PROCEDURE

2.1 Preparation of composite coatings

H13 die steel was selected as the experimental substrate. Each sample had dimensions of (10 × 10 × 5) mm. After having been polished with different-grit sandpapers of 800 # to 2000 #, the samples were ultrasonically cleaned in acetone for 30 min, followed by cleaning with anhydrous ethanol and deionized water, and then fixed onto a sample holder after drying. The sample holder was rotating during heating, etching and deposition. High purity argon (purity of 99.999 %) was used as the protective gas, and nitrogen (purity of 99.99 %) was used as the reaction gas.

A vacuum chamber was vacuumized with a mechanical pump and a molecular pump. The vacuum-chamber temperature was 300 °C. When the vacuum degree was less than 5×10^{-3} Pa, the substrate was etched with an RF ion source. The frame rotated at a speed of 15 Hz, and the Ar gas was introduced into the vacuum chamber. The flow rate of Ar was 0.304 $Pa{\cdot}m^3{\cdot}s^{-1}$ (180 sccm (standard cubic centimeters per minute)), and the vacuum degree was 0.7 Pa. The ion-source voltage was set to 500 V. After closing the ion source, the etching time was 20 min. Cr was deposited on the substrate to create the bottom layer. The flow rate of Ar was kept at 0.202 $Pa{\cdot}m^3{\cdot}s^{-1}$ (120 sccm), and the vacuum degree was 0.5 Pa. The current of the Cr metal target was 100 A, and the bias voltage was 200 V. Then the CrN transition layer was deposited. The Ar gas was switched to N_2 gas, the flow rate was 0.676 $Pa{\cdot}m^3{\cdot}s^{-1}$ (400 sccm) and the vacuum was 1.0 Pa. 15 min after the deposition, the graphite-target baffle of DC magnetron sputtering was opened and a CrCN transition layer was deposited. The Ar flow was 0.202 $Pa{\cdot}m^3{\cdot}s^{-1}$, the N_2 flow was 0.0676 $Pa{\cdot}m^3{\cdot}s^{-1}$, the vacuum was 0.6 Pa, and the graphite-target current was 2.0 A. Finally, a TSiCN nanocomposite coating was deposited using a TiSi target. The duty cycle was 30 %, the current of the TiSi target was 100 A, and the current of the graphite target was 2.5 A. The total flow rates of N_2 and Ar were maintained at 0.405 $Pa{\cdot}m^3{\cdot}s^{-1}$ (240 sccm). Different TiSiCN coatings were prepared by changing the flow ratios of N_2 and Ar, and denoted as Sample 1, Sample 2, Sample 3, Sample 4 and Sample 5. Deposition parameters are shown in **Table 1**.

Table 1: Deposition conditions for TiSiCN coatings

Coatings	Bias (V)	Nitrogen ($Pa·m^3·s^{-1}$) (sccm)	Argon ($Pa·m^3·s^{-1}$) (sccm)	Temperature (°C)	Pressure (Pa)	Time (min)
Sample 1	80	0.0767 (40)	0.338 (200)	350	0.65	80
Sample 2	80	0.1352 (80)	0.270 (160)	350	0.65	80
Sample 3	80	0.202 (120)	0.202 (120)	350	0.65	80
Sample 4	80	0.270 (160)	0.1352 (80)	350	0.65	80
Sample 5	80	0.338 (200)	0.0767 (40)	350	0.65	80

2.2 Test methods

The surface morphology, cross-sectional morphology and wear trajectory of the coating were observed with scanning electron microscopy (SEM). The secondary electron mode was selected in the experiment, with an acceleration voltage of 20 kV and working current of 20 µA. The thickness of the coating was measured with a spherical pit tester and a hardness tester, and the results were more accurate when combined with the cross-sectional morphology analysis. The surface roughness of the coating was tested with a TR100 roughness tester from Time Company. A micro Vickers hardness tester was used to test the hardness of the coatings, and the experimental force was 0.49 N. The binding force was analyzed by a Rockwell hardness tester and a scratch tester, and the scratch morphology was observed with an optical microscope. The indentation load of the diamond head of the hardness tester was 1500 N. The scratch tester was used to scratch the coating surface, and the load was 0–100 N. The phase structure was analyzed with X-ray diffraction (XRD). The measurement range was 20–90°, the tube voltage was 30 kV, the tube current was 2–10 mA, and the scanning step was 2° min^{-1}. The chemical state and content of each element in a coating were tested with X-ray photoelectron spectroscopy (XPS). The high voltage was 12 kV, current was 6×10^{-3} A, and vacuum was 1.067×10^{-5} Pa. The composition and content of each element in a coating were analyzed in accordance with the experimental results of XPS. At the same time, the element content of the wear-trace surface was analyzed to assess the damage mechanism of wear. Annealing experiments at different temperatures were carried out in a box furnace. The samples were heated to the required temperature at a rate of 5 °C/min for 2 h, and then cooled to room temperature in the furnace. The friction coefficients of different coatings were obtained with a multifunctional friction and wear tester (UMT-3). A GCr15 ball with a diameter of 6 mm was selected for the experiment. The experimental load was 2 N and the loading time was 60 min.

3 RESULTS AND DISCUSSION

3.1 Morphologies

Figure 1 shows the surface morphology of different TiSiCN coatings when the N_2/Ar flow ratio increases from 1 : 5 to 5 : 1. **Figures 1a** to **1c** have more large particles. With the increase in the N_2 flow, the number of large particles in **Figures 1d** and **1e** decreases gradually. When the N_2/Ar flow ratio is 1 : 5, the N_2 flow is smaller. The chance of the sputtered particles colliding with the particles in the working atmosphere is reduced, and more

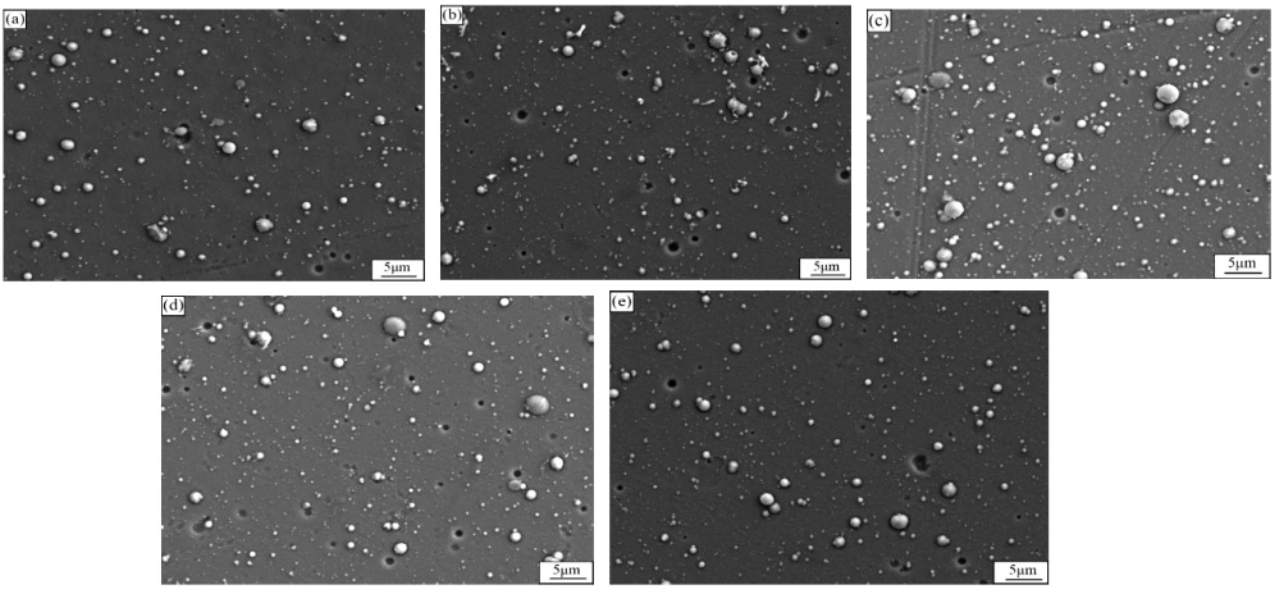

Figure 1: Surface SEM images: a) Sample 1, b) Sample 2, c) Sample 3, d) Sample 4, e) Sample 5

particles are deposited on the coating surface. The particles have a certain bond with the coating and cannot be separated from the coating surface with secondary sputtering. The droplets adhere to the surface of the coating and eventually form more large particles. Moreover, some atoms are deposited directly on the surface of the substrate without the first collision. With the increase in the N_2/Ar flow ratio, the growth of the coating tends to be good. More nitrogen atoms participate in the reaction, improving the crystal quality and the surface quality of the coating.[13,20] When the N_2/Ar flow ratio increases to 5 : 1, the microstructure is uniform and dense, and the surface is the most flat. The reason is that with the increase in the N_2/Ar flow ratio, the reaction process is stable. The particles have enough time to deposit crystals on the surface of the substrate, thereby improving the crystal quality. Therefore, the surface flatness and grain uniformity reach the best state on Sample 5.

Figure 2a shows the cross-sectional morphology, and **Figure 2b** shows the thickness and roughness of the coating. From the cross-section of the coatings, the interface between the transition layer and functional layer can be clearly seen, and the cross-sectional morphology exhibits a featureless structure. When the N_2/Ar flow ratio increases, the thickness of the TiSiCN coating increases from 2.9 µm to 3.39 µm. When the N_2/Ar flow ratio is 1 : 5, the reaction is not sufficient, the prepared coating is thin and the surface is rough. When the N_2/Ar flow ratio is 3 : 3, the roughness decreases and the thickness of the coating reaches the maximum. This is because with the increase in the N_2/Ar flow ratio, the N_2 involved in the reaction increases, the particles can react sufficiently and are deposited on the surface of the substrate. Therefore, the roughness of the coating decreases and the thickness increases. With the increase in the N_2/Ar flow ratio, the roughness first increases and then decreases, and the thickness of the coating increases slightly. This is because the effective contact area between the target and N_2 is determined, limiting the number of deposited particles and the reaction tends to be balanced. The variation trend of the coating thickness is not obvious.[21] When the N_2/Ar flow ratio is 5 : 1, the number of surface defects and large particles is reduced, the structure is dense and the thickness is uniform. The surface roughness is 0.13 µm, and the surface quality of the coating is the best.

3.2 Microstructure

XRD patterns and grain size of the TiSiCN coatings are shown in **Figure 3**. For all the coatings, the crystals belong to Ti (N, C) with multiple orientations of (111) and (200) corresponding to 36.9° and 43.3° in the XRD patterns, respectively. No crystalline phase containing Si was found in the coating. This is because the content of Si is small or exists in an amorphous phase. When the N_2/Ar flow ratio is 3 : 3, the diffraction-peak intensity of the Ti (N, C) (111) plane is the highest, and the grain size becomes larger. When the coating growth is attacked, the Ti (N, C) (111) plane is difficult to destroy, and the crystals prefer to grow along the Ti (N, C) (111) plane. Therefore, with the increase in the N_2/Ar flow ratio, the peak value of the Ti (N, C) (111) plane is enhanced continuously. Due to a thinner thickness of the deposited TiSiCN coating, diffraction peaks of the substrate are detected.[13,19] In addition, Sample 5 shows an obvious Ti (N, C) (200) preferred orientation. The reason is that with the increase in the N_2/Ar flow ratio and C content, it is beneficial to the growth of the (200) crystal plane with higher surface energy, and the intensity of the diffraction peak of Ti (N, C) (200) increases. In this case, the degree of crystallization of the coating is the highest, the crystal is improved, and the hardness is increased.

When the N_2/Ar flow ratio increases from 1 : 5 to 3 : 3, the grain size increases gradually. The reason is that the flow of N_2 is low and there are not enough nitrogen atoms to participate in the reaction. When the N_2/Ar flow ratio is 3 : 3, the grain size is the largest. When the N_2/Ar flow ratio is 5 : 1, the growth condition for the coating tends to be good, the grain size becomes smaller, and the crystallization quality is improved.[20,22] With the

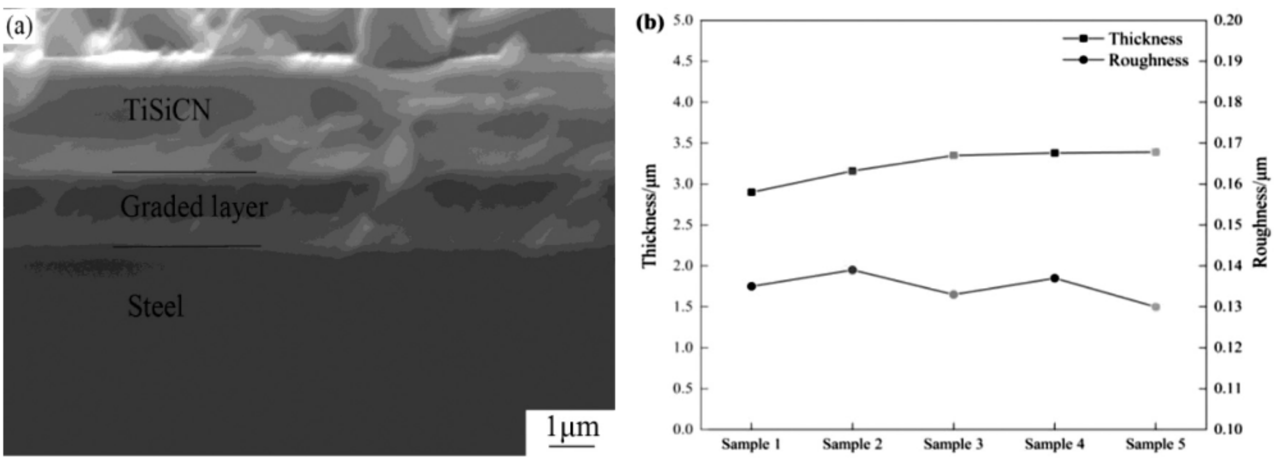

Figure 2: a) Cross-sectional morphology, b) Thickness and roughness of TiSiCN coatings

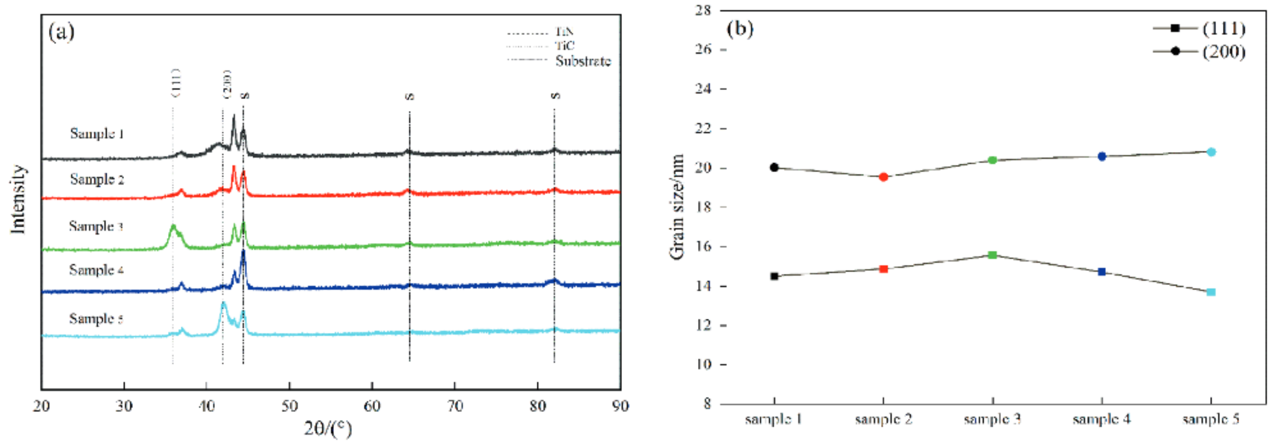

Figure 3: a) X-ray diffraction patterns and b) grain size of TiSICN coatings

increase in the N_2/Ar flow ratio, the grain size first increases and then decreases. However, the difference between different coatings is small, indicating that the N_2/Ar flow ratio has little effect on the grain size of the TiSiCN coatings.

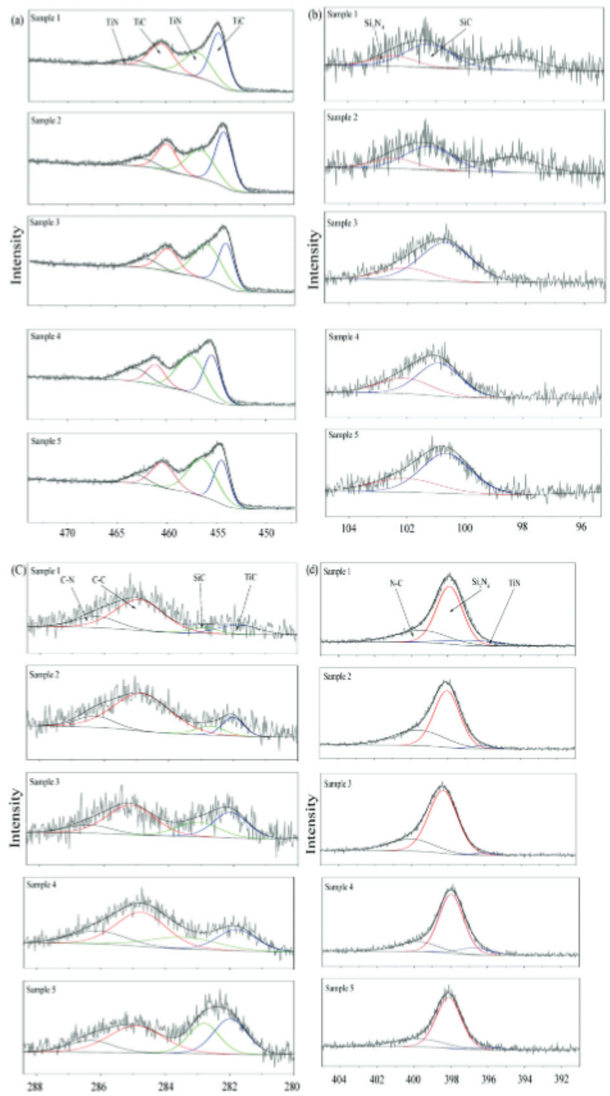

Figure 4: XPS core level spectra: a) Ti 2p, b) Si 2p, c) C 1s, d) N 1s

The elemental chemical state of the TiSiCN coating is characterized with XPS. The XPS spectra of C 1s, Ti 2p, Si 2p and N 1s are shown in **Figure 4**. In the Ti 2p diagram, TiN appears at binding energies of 456 eV and 462 eV, and TiC appears at binding energies of 454 eV and 460 eV. At binding energies of 100.8 eV and 101.8 eV, the peaks corresponding to the Si_3N_4 and SiC bonds appear in the Si 2p spectra. With the increase in the N_2/Ar flow ratio, the content of N increases, leading to an increase in the Si_3N_4 content. The C 1s spectra shows that at (281.8; 282.8; 284.8; 286.4) eV, C exists in the form of TiC, SiC, C-C and C-N bonds, respectively. The C element is mainly amorphous, which may play a role in reducing the friction. But it is not detected in the XRD pattern, which may be due to its low content. The peaks at (396.2; 398.2; 399.8) eV in the N 1s spectrum are attributed to TiN, Si_3N_4 and N-C bonds, respectively. The above conclusions are also consistent with the results from other sources.[15,18] With the increase in the N_2/Ar flow ratio, the content of nitride in the coating increases significantly. In summary, the crystalline phases in the TiSiCN coating are TiN and TiC, and the amorphous phases are SiC, Si_3N_4 and carbon.

The contents of all the elements analyzed based on the XPS results are shown in **Table 2**. The content of nitrogen increased from 28.61 % to 39.15 %, and the content of titanium decreased from 44.38 % to 28.27 %; the content of carbon has no obvious changing trend, and the content of silicon increased slightly. This is because silicon is a semiconductor. The sputtering rate of silicon is usually lower than that of titanium, and the rate control of silicon in a nitrogen environment is difficult. Therefore, when the N_2 flow rate increases, the concentration of nitrogen in the coating increases as expected, while the concentration of silicon hardly changes. In the deposition process, the ionization degree of nitrogen is higher than that of argon, so when the N_2/Ar flow ratio increases, the concentration of nitrogen ions per unit volume increases, and the content of nitrogen in the coating

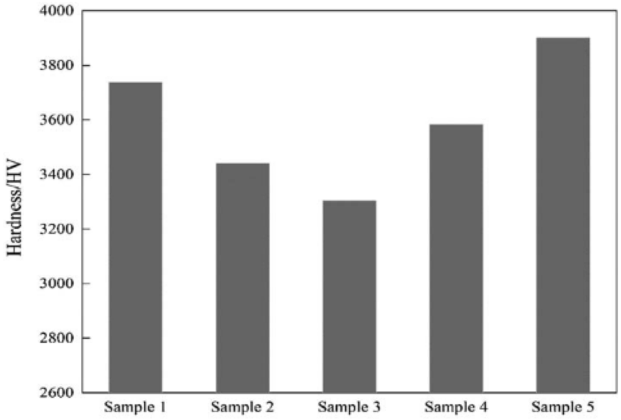

Figure 5: Hardness of TiSICN coatings

also increases. With the increase in the N_2/Ar flow ratio, the particle mass of nitrogen ions is smaller than that of argon ions, and the metal atoms of the target are more difficult to be sputtered by ionized ions. More active nitrogen ions may be combined with the sputtering elements at a higher N_2/Ar flow ratio until the nitrogen in the nitride crystal approaches the saturation capacity.[21] Therefore, the Sample 5 coating has the highest content of nitrogen.

Table 2: Elemental compositions of TiSiCN coatings

Coatings	Chemical composition (*w*/%)			
	Ti	Si	C	N
Sample 1	44.38	19.03	7.98	28.61
Sample 2	40.38	20.41	7.02	32.19
Sample 3	36.96	22.72	6.54	33.78
Sample 4	32.77	22.16	7.48	37.59
Sample 5	28.27	23.04	9.54	39.15

3.3 Mechanical properties

Figure 5 shows the microhardness of TiSiCN coatings, indicating that the hardness of the coating first decreases and then increases. When the N_2/Ar flow ratio is 1 : 5, the microhardness of the coating is 3738.88 HV. When the N_2/Ar flow ratio reaches 3 : 3, the microhardness of the coating reaches a minimum of 3305.01 HV. When the N_2/Ar flow ratio continues to increase to 5 : 1, the coating hardness increases to a maximum of 3902.87 HV. The N_2/Ar flow ratio affects the surface morphology, mechanical properties, and hardness of the coating. When more N_2 is introduced, the reaction is more complete, the surface is smoother and denser, and the grains are refined gradually. The grains of the coating are finer, the grain boundary area is larger. The grain boundaries are more tortuous, the propagation of cracks is less conducive and the hardness of the coating is higher. The structure is denser, the surface defects is fewer and the hardness of the coating is higher.[15,19] Therefore, Sample 5 has the highest hardness.

The bonding strength of the TiSiCN coatings was qualitatively analyzed in accordance with the Rockwell indentation law, and the results are shown in **Figure 6**. When the N_2/Ar flow ratio is 1 : 5, a small amount of cracks can be found around the indentation. With the increase in the N_2/Ar flow ratio, the number of cracks around the indentation gradually decreases. When the N_2/Ar flow ratio is 3 : 3, there is no crack around the indentation, and the bonding strength is the best. When the N_2/Ar flow ratio increases to 5 : 1, a small amount of cracks reappear around the indentation. This is because with the gradual increase in the N_2/Ar flow ratio from 3 : 3 to 5 : 1, the content of nitride in the coating increases significantly, making the coating hard and brittle. When the coating is subjected to the compressive stress of the pressure head of the hardness tester, cracks are more likely to occur. Therefore, with the increase in the N_2/Ar flow ratio, the bonding strength of the coating first increases and then decreases. The bonding strength of Sample 2 is HF-4, the bonding strength of Samples 1, 4 and 5 is HF-3, and the bonding strength of Sample 3 is HF-2.

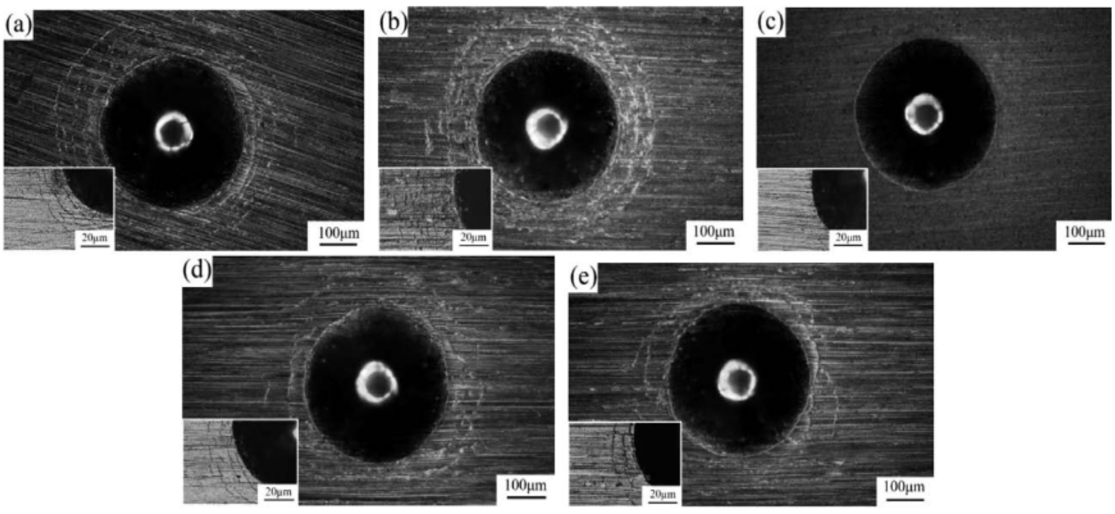

Figure 6: Surface failures due to indentation tests for a binding-force evaluation: a) Sample 1, b) Sample 2, c) Sample 3, d) Sample 4, e) Sample 5

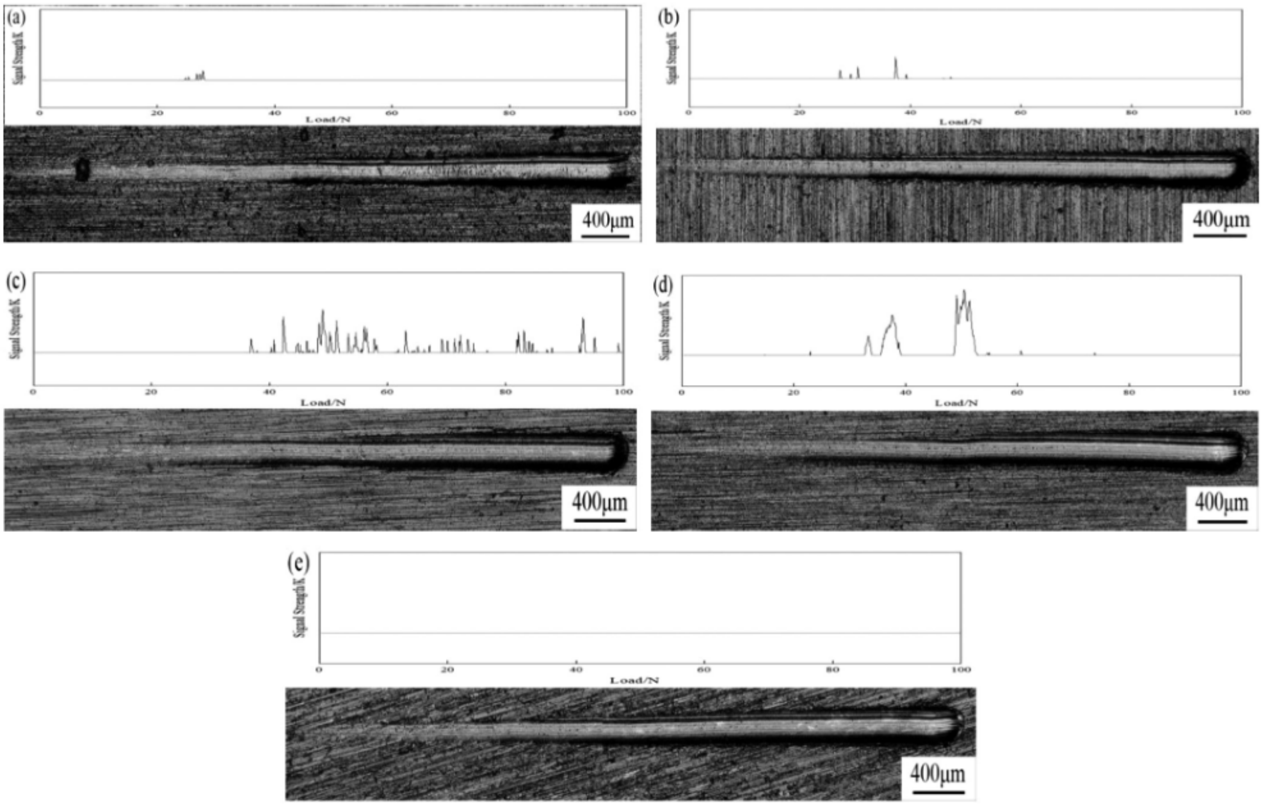

Figure 7: Scratch-test morphology and acoustic emission signal curve: a) Sample 1, b) Sample 2, c) Sample 3, d) Sample 4, e) Sample 5

Figure 7 shows the morphology of scratches. The film/substrate binding force of the TiSiCN coating first decreases and then increases. The formation of each crack or debris produces an acoustic signal peak. When the N_2/Ar flow ratio is 1 : 5, the binding force of the coating is improved; only a small number of cracks appear at the edges of the scratch, and the acoustic emission signal fluctuates slightly. This is because with a lower content of N_2 in the coating, the deposited particles can obtain higher kinetic energy, accelerate the deposition to the substrate surface, eliminate some internal defects, and obtain a dense structure and excellent binding force. With the increase in the N_2/Ar flow ratio, the binding force decreases gradually, the cracks begin to appear on the edges of and inside the scratch, and the acoustic emission signal gradually becomes dense. This is because most of the particles are deposited directly on the surface of the substrate to form larger particles. As a result, the surface of the coating is rough, and the bonding force of the film base decreases. When the N_2/Ar flow ratio is 5 : 1, the coating has the best binding force, the scratch edges are smooth without any cracks, and the acoustic emission signal is stable without any fluctuations. In this case, the volume of the vacuum chamber is limited, and sufficient N_2 can collide with the particles many times. Secondary sputtering reduces the size of deposited particles and the substrate surface is smoother. So the film/substrate binding force of Sample 5 is the best.

3.4 Tribological performance

Figure 8 shows the results of friction and wear experiments after annealing at room temperature and at (400; 500; 600) °C. The process of friction and wear of the coating is divided into two stages: running-in wear and stable wear. With the increase in the annealing temperature, the friction coefficients of different coatings increased slightly, and the friction-coefficient curve was still stable after annealing at 600 °C. This shows that high temperature has little effect on the tribological properties of coatings. With the increase in the N_2/Ar flow ratio, the friction coefficient first increases and then decreases. The friction coefficients of Samples 3 and 5 are low, the overall fluctuation is small, and the tribological properties are better than those of the other three coatings. When the N_2/Ar flow ratio is 3 : 3, the friction-coefficient curve of the coating annealed at room temperature and 400 °C has little fluctuation. After annealing at different temperatures, the friction coefficient of Sample 5 is the lowest, and the average friction coefficients are 0.5257, 0.5779, 0.5314 and 0.5754, respectively. Sample 5 shows excellent wear resistance, friction reduction and high-temperature stability. This is because with the increase in the N_2/Ar flow ratio, more nitrogen elements participate in the reaction. The quality of crystallization is improved, the surface of the coating is more smooth and dense, and the hardness is higher. At the same time, with the increase in the Si and C content in

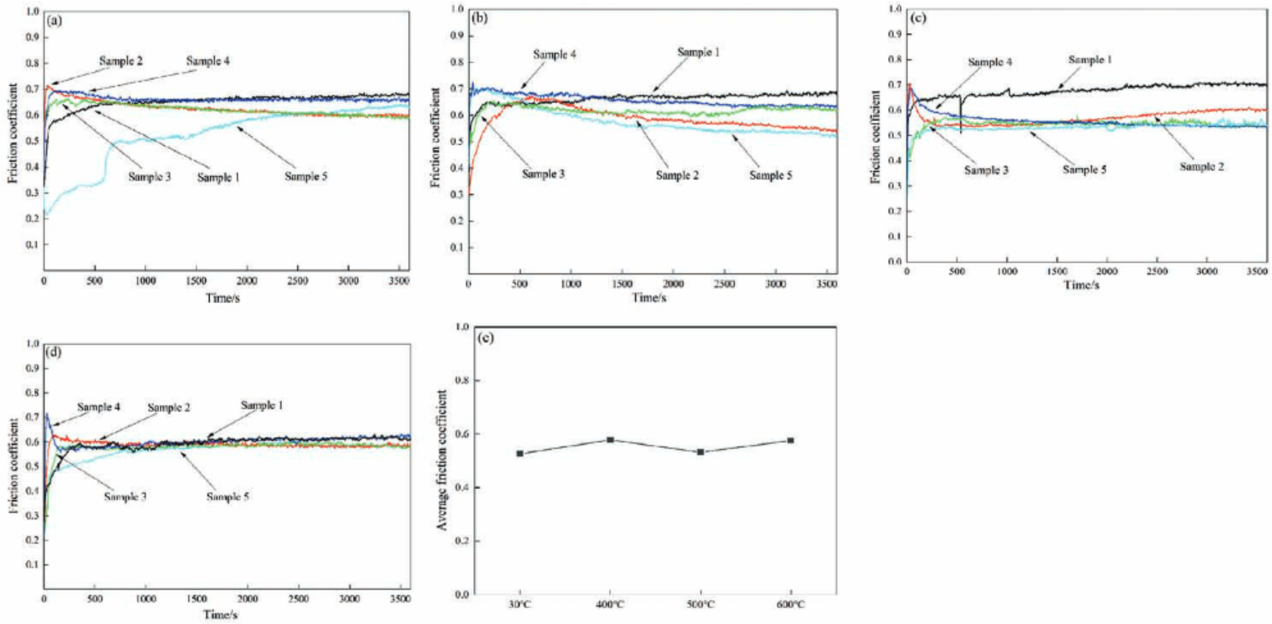

Figure 8: Friction coefficient of TiSiCN coatings: a) 30 °C, b) 400 °C, c) 500 °C, d) 600 °C, e) average friction coefficient of Sample 5

the coating, amorphous C can play a role in friction reduction, reducing the friction coefficient of the coating.[14,21] Therefore, Sample 5 exhibits excellent wear resistance, friction-reduction characteristics and high-temperature stability.

The wear-scar morphologies of different TiSiCN coatings annealed at 500 °C are shown in **Figure 9**. There is no wear debris on the sides of the wear scars, and the wear-scar surfaces are very smooth. With the increase in the N_2/Ar flow ratio, the width of the wear scar first increases and then decreases. The wear-scar widths of Samples 2, 3 and 4 are wide, and the element analysis shows larger O contents on the surfaces. It shows that there are many oxides on the surfaces of the wear scars, and the oxide layers are oxidized and adhered during the peeling process. The debris and grooves parallel to the sliding direction of the coating can be clearly seen, and the wear mechanism includes abrasive wear and adhesive wear. The wear-scar widths of Samples 1 and 5 are narrow, and the O contents on the surfaces are lower. This indicates that there are fewer oxides on the surfaces of the wear scars, and the wear mechanism is the abrasive wear. The wear scar of the coating of Sample 5 is the narrowest and the O content is the smallest; this sample exhibits excellent wear resistance. This is because of the high content of C in Sample 5. Amorphous C can play a role in the lubrication layer on the surface of the wear scar, reducing the friction coefficient and improving the

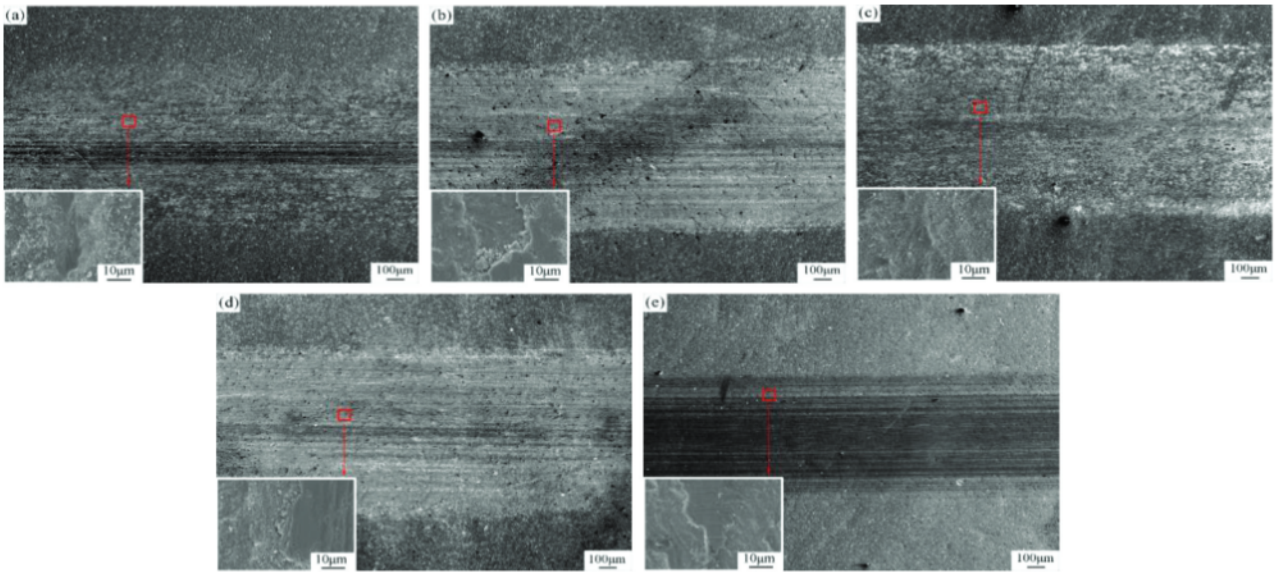

Figure 9: SEM images of the wear scar. a) Sample 1, b) Sample 2, c) Sample 3, d) Sample 4, e) Sample 5

wear resistance. At the same time, with the increase in the N_2/Ar flow ratio, the surface becomes increasingly smoother and denser, while the hardness and binding force increase gradually. The excellent mechanical properties allow the coating to exhibit high wear resistance.[18,28] When the N_2/Ar flow ratio is 5 : 1, the coating has the best high-temperature stability and wear resistance.

4 CONCLUSIONS

The TiSiCN coating was prepared using the composite technology of multi-arc ion plating and magnetron sputtering, and the effect of the N2/Ar flow ratio on various properties of the coating was studied. The results are as follows:

1) With an increase in the N_2/Ar flow ratio, the surface becomes smoother and denser. The thickness of the TiSiCN coating increases gradually. When the N_2/Ar flow ratio is 5 : 1, the number of surface defects and large particles decreases. The surface roughness is the lowest.

2) The XRD pattern clearly shows preferred orientations of Ti (C, N) (111) and Ti (C, N) (200). With the increase in the N_2/Ar flow ratio, the intensity of the TiN (200) diffraction peak increases, and the grain size first increases and then decreases. XPS results show that there are amorphous phases of SiC, Si_3N_4 and C in the coating, and the content of N in the coating increases gradually.

3) When the N_2/Ar flow ratio is 5 : 1, the TiSiCN coating has the highest microhardness and the best binding force. The average friction coefficient after annealing at different temperatures is the lowest. The TiSiCN coating shows excellent wear resistance, friction-reduction performance and high-temperature stability.

Acknowledgment

This work was supported by the Key R&D Projects of the Shandong Province under Grant No. 2019GGX102023.

5 REFERENCES

[1] S. Guha, S. Das, A. Bandyopadhyay, S. Das, Investigation of structural network and mechanical properties of Titanium silicon nitride (TiSiN) thin films, Journal of Alloys and Compounds, 731 (**2018**), 347–53, doi:10.1016/j.jallcom.2017.09.340

[2] Y. Moritz, C. Saringer, M. Tkadletz, A. Starkc, N. Schellc, I. Letofsky-Papstd, C. Czettle, M. Pohlere, N. Schalk, Oxidation behavior of arc evaporated TiSiN coatings investigated by in-situ synchrotron X-ray diffraction and HR-STEM, Surface and Coatings Technology, 404 (**2020**), doi:10.1016/j.surfcoat.2020.126632

[3] Q. Wan, B. Yang, Y. Chen, Y. Cai, Y. Liu, L. Meng, D. Gao, Effect of bilayer period on microstructure and mechanical properties of TiSiN/TiN coatings, Materialia, 3 (**2018**), 260–264, doi:10.1016/j.mtla.2018.08.027

[4] Y. Ye, Y. Yao, H. Chen, S. Guo, J. Li, L. Wang, Structure, mechanical and tribological properties in seawater of multilayer TiSiN/Ni coatings prepared by cathodic arc method, Applied Surface Science, 493 (**2019**), 1177–86, doi:10.1016/j.apsusc.2019.07.140

[5] Y. B. Zhu, M. Dong, J. Li, L. Wang, Wear failure mechanism of TiSiN coating at elevated temperatures, Applied Surface Science, 487 (**2019**), 349–55, doi:10.1016/j.apsusc.2019.05.120

[6] N. Marchin, F. Ashrafizadeh, Effect of carbon addition on tribological performance of TiSiN coatings produced by cathodic arc physical vapour deposition, Surface and Coatings Technology, 407 (**2021**), doi:10.1016/j.surfcoat.2020.126781

[7] M. Guo, Y. Liang, M. Cai, J. Nie, M. Ju, M. Liu, G. Jiang, Improved slag resistance of taphole clay due to in situ formation of TiCN from ferrotitanium slag, Ceramics International, 47 (**2021**), doi:10.1016/j.ceramint.2021.05.082

[8] Y. Qin, H. Zhao, C. Li, J. Lu, J. He, Effect of heat treatment on the microstructure and corrosion behaviors of reactive plasma sprayed TiCN coatings, Surface and Coatings Technology, 398 (**2020**), doi:10.1016/j.surfcoat.2020.126086

[9] G. Xian, J. Xiong, H. Zhao, L. Xian, H. Fan, Z. Li, H. Du, Study on the growth and wear behavior of the TiAlN-based composite coating deposited on TiCN-based cermets with different binder phase, Wear, (**2020**), 460–461, doi:10.1016/j.wear.2020.203460

[10] G. Zheng, Q. Jiao, C. Li, Y. Ding, J. He, Y. Jiang, H. Zhao, Influence of nitridation on the microstructure and corrosion behavior of reactive plasma sprayed TiCN coatings, Surface and Coatings Technology, 396 (**2020**), doi:10.1016/j.surfcoat.2020.125954

[11] J. Liu, X. Ji, Z. Guo, C. Qin, Y. Xiao, Q. You, Characteristics and cutting perfomance of the CVD coatings on the TiCN-based cermets in turning hardened AISI H13 steel, Journal of Materials Research and Technology, 9 (**2020**) 2, 1389–1399, doi:10.1016/j.jmrt.2019.11.065

[12] H. Sun, A. Billard, H. Luo, W. Zheng, X. Zheng, M. Dai, S. Lin, Q. Shi, F. Sanchette, Influence of carbon content on the mechanical properties of TiCN–Cu nanocomposite coatings prepared by multi-arc ion plating, Vacuum, 187 (**2021**), doi:10.1016/j.vacuum.2021.110139

[13] M. Dong, Y. Zhu, C. Wang, L. Shan, J. Li, Structure and tribocorrosion properties of duplex treatment coatings of TiSiCN/nitride on Ti6Al4V alloy, Ceramics International, 45 (**2019**) 9, 12461–12468, doi:10.1016/j.ceramint.2019.03.180

[14] A. Hatem, J. Lin, R. Wei, R. Torres, C. Laurindo, G. Souza, P. Soares, Tribocorrosion behavior of low friction TiSiCN nanocomposite coatings deposited on titanium alloy for biomedical applications, Surface and Coatings Technology, 347 (**2018**), 1–12, doi:10.1016/j.surfcoat.2018.04.049

[15] J. Li, Y. Wang, Y. Yao, Y. Wang, L. Wang, Structure and tribological properties of TiSiCN coating on Ti6Al4V by arc ion plating, Thin Solid Films, 644 (**2017**), 115–119, doi:10.1016/j.tsf.2017.09.053

[16] Q. Li, F. Jiang, Y. Leng, R. Wei, N. Huang, Microstructure and tribological properties of Ti(Cr)SiCN coating deposited by plasma enhanced magnetron sputtering, Vacuum, 89 (**2013**), 168–173, doi:10.1016/j.vacuum.2012.03.053

[17] Y. Ma, J. Yang, X. Tian, C. Gong, W. Zheng, Y. He, H. Li, Z. Gao, K. Zhang, L. Wei, P. Chu, Enhanced discharge and surface properties of TiSiCN coatings deposited by pulse-enhanced vacuum arc evaporation, Surface and Coatings Technology, 403 (**2020**), doi:10.1016/j.surfcoat.2020.126413

[18] Y. Wang, J. Li, C. Dang, Y. Wang, Y. Zhu, Influence of carbon contents on the structure and tribocorrosion properties of TiSiCN coatings on Ti6Al4V, Tribology International, 109 (**2017**), 285–296, doi:10.1016/j.triboint.2017.01.002

[19] H. Du, H. Zhao, J. Xiong, W. Wan, Y. Wu, L. Wang, G. Xian, Effect of Ar/N_2 flow ratio on oxidation resistance and properties of TiAl(La)N coatings, International Journal of Refractory Metals and Hard Materials, 46 (**2014**), 173–80, doi:10.1016/j.ijrmhm. 2014.06.012

[20] H. Tian, L. Feng, Z. Liu, Effect of N_2/Ar flow ratio on the structural and electrical properties of SrHfON thin films prepared by magnetron sputtering, Vacuum, 109 (**2014**), 139–143, doi:10.1016/j.vacuum.2014.07.005

[21] G. Xian, H. Zhao, H. Fan, H. Wang, H. Du, The structure and properties of ZrAl(Y)N coatings deposited at various N_2/Ar flow ratios, International Journal of Refractory Metals and Hard Materials, 44 (**2014**), 60–67, doi:10.1016/j.ijrmhm.2014.01.014

[22] X. Zhang, J. Jiang, J. Lin, J. Moore, Effect of N_2 flow on low carbon TiAlNC coatings, Surface and Coatings Technology, 203 (**2009**) 22, 3450–3453, doi:10.1016/j.surfcoat.2009.05.010

[23] X. Li, C. Wang, C. Chen, M. Jiang, X. Hu, Thickness-controllable diamond films deposited on stainless steel using a Cr/Cr-Si-N interlayer prepared at different N_2/Ar flow ratios, Applied Surface Science, 532 (**2020**), doi:10.1016/j.apsusc.2020.147402

[24] J. Yang, X. Meng, C. Yang, W. Fu, Influence of N_2/Ar-flow ratio on crystal quality and electrical properties of ScAlN thin film prepared by DC reactive magnetron sputtering, Applied Surface Science, 282 (**2013**), 578–582, doi:10.1016/j.apsusc.2013.06.014

[25] Q. Guo, Y. Guo, D. Guo, Z. Yang, J. Li, W. Yang, Y. Yang, P. Gao, Y. Bai, Microstructure and properties of the Cp/AlSn coatings deposited by magnetron sputtering/multi-arc ion plating, Surface and Coatings Technology, 384 (**2020**), doi:10.1016/j.surfcoat.2019.125303

[26] X. Ren, R. Zhao, W. Wang, X. Song, Y. Zhang, C. Zhang, Corrosion Resistance of TiCN Films Prepared with Combining Multi-arc Ion Plating and Magnetron Sputtering Technique, Rare Metal Materials and Engineering, 47 (**2018**) 7, 2028–2036, doi:10.1016/s1875-5372(18)30176-0

[27] R. Zhao, X. Ren, K. Wen, H. Liu, M. Huang, Z. Wang, Y. Deng, Multi-arc ion plating and DC magnetron sputtering integrated technique for high-performance Al,C-co-doped d-TiN quaternary films, Corrosion Science, 182 (**2021**), doi:10.1016/j.corsci.2021.109261

[28] Y. Wang, J. Li, C. Dang, Y. Wang, Y. Zhu, Influence of bias voltage on structure and tribocorrosion properties of TiSiCN coating in artificial seawater, Materials Characterization, 127 (**2017**), 198–208, doi:10.1016/j.matchar.2017.03.012